Multixenobiotic resistance in Mytilus edulis: Molecular and functional characterization of an ABCG2- type transporter in hemocytes and gills

Yosra Ben Cheikh, Benoît Xuereb, Céline Boulange-Lecomte, Frank Le Foll

Multixenobiotic resistance in *Mytilus edulis*: molecular and functional characterization of an ABCG2- type transporter in hemocytes and gills

Yosra Ben Cheikh[a], Benoit Xuereb[a], Céline Boulangé-Lecomte[a] and Frank Le Foll[a]

Authors affiliation

[a]University of Le Havre Normandy, Environmental Stress and Aquatic Biomonitoring, UMR-I 02 SEBIO, 25 rue Philippe Lebon, F-76063 Le Havre, France

Corresponding Author

Yosra Ben Cheikh

E-mail: yosra_bencheikh@yahoo.fr

Tel +33 (0)2 32 74 43 79

Abstract

Among the cellular protection arsenal, ABC transporters play an important role in xenobiotic efflux in marine organisms. Two pumps belonging to B and C subfamily has been identified in *Mytilus edulis*. In this study, we investigated the presence of the third major subtype ABCG2/BCRP protein in mussel tissues. Transcript was expressed in hemocytes and with higher level in gills. Molecular characterization revealed that mussel ABCG2 transporter share sequence and organizational structure with mammalian and molluscan orthologs. Overall identity of the amino acid sequence with corresponding homologs from other organisms was comprised between 49% and 98%. Furthermore, protein efflux activity was demonstrated using a combination of fluorescent allocrites and specific inhibitors. The accumulation of bodipy prazosin and pheophorbide A was heterogeneous in gills and hemocytes. Most of the used blockers enhanced probe accumulation at different levels, more significantly for bodipy prazosin. Moreover, Mrp classical blocker MK571 showed a polyspecificity.

In conclusion, our data demonstrate that several ABC transporters contribute to MXR phenotype in the blue mussel including ABCG2 that form an active pump in hemocytes and gills. Efforts are needed to distinguish between the different members and to explore their single function and specificity towards allocrites and chemosensitizers.

Keywords: ABC transporter, efflux activity, blue mussel, invertebrates

1. Introduction

The aquatic environment is polluted by a variety of chemical compounds and heavy metals released by urban communities and industrial plants. Many of these xenobiotics are known to be a threat to most marine species health due to their environmental persistence, bioaccumulation in various tissues and intrinsic toxicity (Anita H Poulsen, 2012; Giarratano et al., 2010). Bivalves of the genus *Mytilus* are of particular interest because of their resistance to chemical contaminants. These bioindicator species are therefore used as sentinel organisms. Immunological responses mediated by hemocytes are frequently investigated to monitor biological effects of water pollution (Akaishi et al., 2007; Auffret et al., 2006; Gupta and Singh, 2011).

In order to survive, marine organisms have developed strategies to overcome adverse effects of pollutants. Bivalves can limit their exposure to toxic compounds using behavioural responses such as shell closure and restriction of filtration rate (Haberkorn et al., 2011; Hégaret et al., 2007). Furthermore, they possess multiple cellular detoxification mechanisms that can influence the uptake, distribution and elimination of xenobiotics (Farris and Hassel, 2006). Among the arsenal of enzymes involved in animal cell detoxification, some members of the ATP Binding Cassette (ABC) superfamily are found (Bard, 2000; Luckenbach et al., 2008; Rioult et al., 2014).

ABC transporters were first described for their role in multidrug resistance (MDR) to chemotherapeutic drugs (Gottesman and Ling, 2006; Nielsen and Skovsgaard, 1992; Sharom, 2008). These ATP-powered transmembrane proteins found in tumor cells of mammals are one of the major cause of chemotherapeutic failure in cancer therapy. They actively pump out of the cytosol into the external medium a multitude of distinct cytotoxic compounds (Kathawala et al., 2015). Similarly to this efflux-based drug resistance, a xenobiotic transport mediated by ABC proteins was demonstrated for the first time in fresh water mussels as a strategy to defense against pollutants (Kurelec, 1992; Kurelec and Pivcević, 1989). Considering the variety of chemically unrelated compounds carried by this system, Kurelec coined the term of Multixenobiotic Resistance (MXR) by analogy to the MDR phenotype (Kurelec, 1992). In marine organisms, ATP-fueled pumps act as a first line of defense, preventing toxic chemicals from entering the cell. Secondarily, if toxicants even enter the cytoplasm, ABC transporters can be the last protection by expelling the toxicants and associated metabolites (Epel et al., 2008).

The MXR phenotype is supposedly ubiquitous in aquatic invertebrates. Functional and molecular assays allowed the identification and characterization of some ABC transporters

members in several species including sponges (Kurelec et al., 1992), innkeeper worms (Toomey and Epel, 1993), molluscs (Faria et al., 2011; Luckenbach and Epel, 2008; McFadzen et al., 2000; Navarro et al., 2012; Rioult et al., 2014) and crabs (Köhler et al., 1998; Minier et al., 2008).

The three major types of MDR proteins in humans include members of the ABCB, the ABCC and the ABCG2 subfamilies (Sarkadi et al., 2006). In marine invertebrates, only ABCB and ABCC transporters have been well described. Two complete sequences analog to ABCB/P-glycoprotein (P-gp) and ABCC/MDR-related protein (MRP) subfamilies were identified in Californian mussel (Luckenbach and Epel, 2008). Furthermore, efflux activities have been confirmed using functional efflux assays with substrates and inhibitors (Luckenbach et al., 2008; Luckenbach and Epel, 2008). Similarly, P-gp transcript as well as pump activity were characterized in the Asian green mussel *Perna viridis* (Huang et al., 2014). In *Mytilus edulis*, Luedeking and co-authors obtained fragments of abcb and abcc sequences in various tissues and MXR transcript levels were measured in gills, mantle and digestive gland (Luedeking et al., 2005; Luedeking and Koehler, 2002). Lately, ABCC/MRP transporter was detected in blue mussel hemocytes. Authors demonstrated that pump activity was principally supported by the hemocyte subpopulation eosinophilic granulocytes (Rioult et al., 2014). To our knowledge, only few studies explored the presence of ABCG2/BCRP transporter in bivalves. Protein and gene expression were quantified respectively in the Indian rock oyster *Saccostrea forskali* (Kingtong et al., 2007) and the Asian clam *Corbicula fluminea* (Chen et al., 2015).

In this study, we investigate the existence of the third major type of MDR proteins ABCG2 in blue mussel hemocytes and gills. Complete ABCG2 amino acid sequence was identified and characterized. Therefore, ABCG2 gene expression was quantified and transcript levels were compared in mussel tissues. For determining whether ABCG2 transporter is active in *M. edulis* hemocyte subpopulations and gills, dye efflux assays were performed using fluorescent substrates combined with specific blockers.

2. Material and methods

2.1. Chemicals

Bodipy prazosin (Invitrogen Life technologies) and pheophorbide A (Sigma Aldrich) were used as fluorescent dyes and substrates of BCRP. Inhibitors of ABC transporters described in **Table 1** were purchased from Sigma Aldrich and Tebu-bio for Ko134.

2.2. Mussel and tissue collection

Adult mussels, *M. edulis* with shell length ranging from 4 to 5 cm, were collected on the intertidal rocky shore of Yport (0°18'52"E:49°44'30"N, France) between April 2014 and December 2015, immediately transported to the laboratory and placed in a temperature-controlled (10°C) aerated Biotop Nano Cube 60 seawater tank (Sera, Heinsberg, Germany), equipped with mechanical and activated biological filtering. The animals were fed with algae (*Isochrysis galbana*) and maintained in these conditions for at least one week before use.

Hemolymph was withdrawn from the posterior adductor muscle sinus, by gentle aspiration with a 1 mL syringe equipped with a 22G needle. For RNA extraction, pooled aliquots from 10 mussels were centrifuged 5 min at 1200 g. Gills were gently removed from mussel and immediately used in RNA extraction. For efflux activity assays, tissues were kept entire or excised using biopsy punches (6 mm diameter) to obtain disks.

2.3. RNA extraction and cDNA synthesis

Total RNA was isolated from hemocytes or from gills using RNeasy mini kit (Qiagen) according to the manufacture's recommendations. RNA suspensions were treated with DNase (Turbo DNA free kit, Ambion) for genomic DNA removal. Total RNA concentration was analyzed by spectrophotometry (Nanodrop, Thermo Scientific). RNA integrity was checked by electrophoresis on 1 % agarose gel with SYBR staining (SYBR Safe DNA gel stain, Invitrogen). Reverse transcription was carried from total RNA (1 µg) using M-MLV RNAse H minus (100U, Promega) and oligo$(dT)_{20}$ (1 µg) in the presence of Recombinant RNasin® Ribonuclease Inhibitor (80U, Promega). Complementary first-strand DNA (cDNA, 40 µL) were diluted in 60 µL of ultra-pure water and stored in 5 µL aliquots at -20°C until use.

2.4. Gene fishing and analysis of transporter sequence

The primers used in gene fishing were directed against sequence of abcg2 ortholog from *Mytilus galloprovincialis* (Genbank accession number gi|406717747) and designed using Primer3 software (http://bioinfo.ut.ee/primer3-0.4.0/, **Table 2**). PCR was performed on cDNA gills using Taq'Ozyme purple mix (Ozyme). After an initial denaturation step at 95°C for 2 min, 45 cycles were performed including a denaturation step at 95°C for 30 s, annealing at 62°C for 30 s and extension at 72°C for 1 min. The final extension step was continued for 5 min. The amplified PCR products were purified from 1.2% agarose gel using QIAquick gel extraction kit (Qiagen). Partial cDNA sequences were obtained after sequencing and blasted with abcg2 cDNA from other organisms to verify the homology (https://blast.ncbi.nlm.nih.gov/Blast.cgi).

The 5' cDNA of *Mytilus edulis* abcg2 was obtained by 5'RACE PCR using SMART RACE cDNA amplification kit (Clontech) according to the user's manual. The 5'RACE product was amplified by PCR using gene specific primer (**Table 2**) and universal primer mix supplied with the RACE PCR kit. PCR was performed in a touchdown mode: 5 cycles at 94°C (30 s)/72°C (3 min), 5 cycles 94°C (30 s)/70°C (30 s)/72°C (3 min) and 25 cycles 94°C (30 s)/68°C (30 s)/72°C (3 min). Amplified products were gel purified, cloned and sequenced. The resulting PCR and RACE PCR sequences were assembled using Geneious R7.1.9 software. In order to get the whole open reading frame and to confirm assembled sequences, a PCR reaction was performed using primers directed against *Mytilus edulis* abcg2 (**Table 2**) following the same cycling conditions cited previously.

Final sequence was analyzed using tools at expasy (http://web.expasy.org/), NCBI (http://www.ncbi.nlm.nih.gov/) and cbs server (http://www.cbs.dtu.dk/services/). Multiple sequence alignment and determinations of identity rates between amino acid sequences of ABC transporters from different organisms were performed using Clustal W2. Phylogenetic tree was built according to Neighbor-Joining method using Geneious R7.1.9 software.

2.5. Quantitative real-time polymerase chain reaction

QPCR analysis was conducted on the Rotor-Gene Q 2- plex HRM (QIAGEN, Courtaboeuf, France) using the QuantiTect® SYBR® Green Master Mix (2X, QIAGEN). Each reaction was run in duplicate with a final volume of 20 µL containing 5 µL cDNA and 0.5 µM of each primer. Specific qPCR primers for abcg2-like and the housekeeping (hk) Elongation factor *ef1α* were designed using ProbeFinder software (https://lifescience.roche.com/, **Table 2**). The *ef1α* was chosen as hk gene because of its stability from different experimental conditions (Lacroix et al., 2014).

Reactions were initiated with an initial denaturation for 15 min at 95 °C followed by 45 cycles at 94 °C for 15 s, 59 °C for 30 s and 72 °C for 6 s. The melting curve was finally determined during a slow temperature elevation from 60 to 95 °C (1°C.s^{-1}). The run included blank controls (water). For the qPCR efficiencies of each primer pair used, standard curves were generated using eight serial dilutions of cDNA (from 10^9 to 10^1 copies) (Xuereb et al., 2012). The level of expression of the target genes, normalized to the *ef1α* housekeeping gene, was then calculated using the $(1+\text{efficiency})^{-\Delta Ct}$ formula.

182 **2.6. Analysis of MXR activity**

183 MXR activity was assessed in hemocytes by flow cytometry and in gills by microplate reader
184 assays using dye efflux assays in absence or presence of inhibitors.

185 **2.6.1. MXR activity in hemocytes**

186 Crude hemolymph was placed into individual wells of 24-well tissue-culture plates (Greiner)
187 and cells allowed to adhere for 15 minutes at 15 °C. The hemolymph was removed and replaced
188 with 400 µL of marine physiological saline solution (MPSS, pH 7.8, 0.2 µm filtered) alone for
189 the control or containing ABC transporter inhibitors at 30 µM final concentration. After 30 min
190 of incubation at 15°C, fluorescent dyes were added: pheophorbide A at 5 µM or bodipy prazosin
191 at 0.5 µM and incubated 15 min at 15 °C. Supernatants were gently aspirated and attached cells
192 were removed by adding cold Alsever's solution (300 mM NaCl, 100 mM Glucose, 30 mM
193 sodium Citrate, 26 mM citric acid, 10 mM EDTA, pH 5.4) and immediately analyzed by Cell
194 Lab Quanta SC MPL flow cytometer (Beckman Coulter).

195 **2.6.2. MXR activity in gills**

196 Entire gills or tissue disks obtained by biopsy punches, were placed into individuals wells of
197 12-well plates (Greiner) or black 96-well plates (nunc) filled with MPSS. ABC transporter
198 inhibitors were added at 30 µM and incubated for 30 min at 15 °C. Thereafter, pheophorbide A
199 (5 µM) or bodipy prazosin (0.5 µM) were added for 15 min at 15 °C. Whole gills or tissue
200 disks were transferred in new wells containing MPSS to remove the probe excess and
201 homogenized by horizontal rotation for 30 s. The fluorescence accumulated was measured with
202 a microplate reader (Tecan, excitation/ emission wavelength in nm: 490/530 for bodipy
203 prazosin and 395/670 for pheophorbide A).

204 Mean values of fluorescence measured from biopsies were plotted and compared. A MXR
205 activity factor (MAF) was calculated using the following formula: $100 * \left(\frac{\text{MFL inhibitor - MFL ctrl}}{\text{MFL inhibitor}}\right)$
206 wherein $MFL_{inhibitor}$ and MFL_{ctrl} are the mean fluorescence intensity values measured in the
207 presence and absence of inhibitor (Lebedeva et al., 2011).

208 **2.7. Statistical analyses**

209 Statistical analysis was performed by using SigmaPlot 12 (Systat Software Inc., Chicago, IL).
210 Replicates were averaged and the values were tested for normality (Shapiro-Wilk) and paired
211 comparisons were performed by Student's t-tests. Statistical significance was accepted for $*p < 0.05$, $**p < 0.01$ or $***p < 0.001$.
212

213 **3. Results**

214 **3.1. Identification and phylogenetic analysis of ABCG2 transporter**

215 The expression of ABCG2 gene in *Mytilus edulis* gills was investigated by RT PCR. The
216 amplified product had the expected size and generated a partial cDNA sequence of 542 pb.
217 Blast analysis confirmed that the fragment was a part of an abcg2-like gene sequence.

218 The 2198 pb full length cDNA sequence was secondarily obtained by assembling of various
219 sequences from RACE and PCR reactions performed on different cDNAs (Genbank accession
220 number KX551963). It contained a 1926 pb ORF encoding a 641 amino acid polypeptide. In
221 addition, 265 pb and 6 pb of 5'-and 3'-UTR were identified. The deduced amino acid sequence
222 has a calculated molecular mass of 71.5 kDa and a theoretical isoelectric point of 7.57.

223 Analyses of amino acid sequence revealed the structural organization of ABCG2 transporter in
224 a single subunit with a nucleotide binding domain (NBD) and a membrane spanning domain
225 (MSD). The NBD contained highly conserved motifs of ABC transporters: the walker A/P-
226 loop, walker B, ABC signature (C motif) as well as the Q-loop/lid upstream of the walker A
227 and the D-loop and H-loop/switch regions downstream of the walker B (**Figure 1-2**).
228 Furthermore, the MSD was organized in six putative transmembrane helices and the NH_2
229 terminal was located in the cytosol. Two possible N-glycosylation sites (Asn-Val-Ser) were
230 identified respectively in the 2^{nd}-3^{rd} (amino acid 454-456) and the 5^{th}-6^{th} (amino acid 552-554)
231 transmembrane helice. No signal peptide was detected (**Figure 1-2**).

232 The phylogenetic analysis revealed the similarity of *M. edulis* ABCG2 with other representative
233 ABCG2 protein from different species (**Figure 3**). *M. edulis* amino acid sequence matched the
234 most with *Mytilus galloprovincialis* (98%), *Crassostrea gigas* (65%) and *Lottia gigantea*
235 ABCG2 (64%) while identities with other vertebrates and invertebrates orthologs were
236 comprised between 49% and 61% (49% with human protein).

237 **3.2. ABCG2 transcript levels in hemocytes and gills**

238 The expression of *abcg2*-like mRNAs was investigated in *Mytilus edulis* hemocytes and gills (

239 **Figure 4**). Transcript levels were normalized to *ef1α*. This housekeeping gene was stable
240 amongst tissues (data not shown). Both tissues showed the presence of *abcg2*-like gene product.
241 Furthermore, transcripts were significantly more abundant in gills (2.5 times, $p<0.01$) than in
242 hemocytes.

3.3. ABCG2 transporter activity

BCRP efflux activity was investigated in hemocyte suspensions and gill tissues using bodipy prazosin (Cooray et al., 2004) and pheophorbide A (Robey et al., 2004) as ABCG2 pump allocrites. Cells were treated with pharmacological blockers characterized by their specificity for human ABC transporters (**Table 1**).

3.3.1. In hemocytes

BCRP efflux activity was explored in hemocyte subpopulations by flow cytometry. Cell fluorescence was analysed according criteria of cell size (EV expressed in µm) and inner complexity (side-scatter signal). Two non-overlapping regions were defined on EV/SS dot plots. The region R1 corresponds to small semi-granular basophils and the region R2 to large granular and semi-granular cells called eosinophils (**Figure 5**a). The normalized intracellular fluorescence concentration (FL-FC, arbitrary units) was calculated from the ratio of FL to EV (**Figure 5**b).

The cell fluorescence varied according to the probe used. Bodipy prazosin was more accumulated in eosinophils. In contrary, pheophorbide A was slightly more concentrated in basophils. In the presence of ABC transporter inhibitors sildenafil, MK571, Ko134 and elacridar, bodipy prazosin accumulation increased significantly in hemocytes particularly in eosinophils ($p<0.01$ for MK571 and $p<0.001$ for the other blockers), while pranlukast had no effect on dye efflux (**Figure 5c**). By contrast, pheophorbide A efflux was only non significantly inhibited by all blockers, at different levels.

To compare blockers effects on pump activity, the multidrug resistance activity factor was determined (**Table 3**). Cells charged with bodipy prazosin showed an increased MAF for most inhibitors (sildenafil, MK571, KPo134, elacridar) compared to hemocytes incubated with pheophorbide A. Furthermore, with bodipy prazosin no differences were noted between hemocyte subpopulations. By contrast, MAF values were less important in basophils loaded with pheophorbide A than in eosinophils.

3.3.2. In gills

ABCG2 pump activity was explored in gills with a microplate reader assay. Only MK571 and Ko134 significantly increased bodipy prazosin accumulation ($p<0.05$), indicating an inhibition of the dye efflux (**Figure 6a**). The other blockers induced a slight but non-significant increase in cell fluorescence. With the probe pheophorbide A, slight fluorescence increases were obtained mainly in gills pre-incubated with sildenafil or ko134, but no inhibitor produced result

significantly different from control measurements. Furthermore, in control conditions, both BCRP allocrites were more effluxed from the anterior-labial part of gills (**Figure 6b**). In the presence of pump blockers (MK571 and Ko134), fluorescence increased and was more concentrated in the center and anterior side of the tissues.

Gills charged with bodipy prazosin showed higher MAF values compared to pheophorbide A. in the presence of Ko134, efflux activity was more important for both fluorescent probes (**Table 4**). However, MK571 showed a high MAF value only for bodipy prazosin.

4. Discussion

ABC transporters play an important role in cell detoxification. The first genome sequencing and analysis of *Mytilus galloprovincialis* recently pointed out Multidrug Associated Genes as significantly overrepresented in this genus (Murgarella et al., 2016)**.** Until now, only B and C subfamilies were identified in the blue mussel. In this study, we expand the knowledge on ABC pump subtypes and investigate the presence of ABCG2 in *Mytilus edulis* tissues. To this purpose, we combined molecular and functional approaches to explore gene expression and pump activity in the gills and hemocytes.

4.1. ABCG2 molecular characterization

ABCG2 amino acid sequence was identified from the gills of *Mytilus edulis* and characterized. It contained typical conserved structural domains of ABC transporter. Characteristic motifs including the Walker A and B motifs are common to many ATP binding proteins while aromatic D, H and Q loops as well as ABC signature are unique to the family (Dean et al., 2001; Linton, 2007). They play an important role in the functioning of the transporter (Linton, 2007). According to the predicted structure*, Mytilus edulis* ABCG2 is a half transporter, with one NBD followed by one MSD and a molecular weight equal to 71.5 KDa which is closely similar to human ABCG2 (Kathawala et al., 2015).

Phylogenetic analysis grouped the identified protein with other ABCG2 members from several species. *Mytilus edulis* ABCG2 was closely related to invertebrate transporters especially *Mytilus galloprovincialis* and *Crassostrea gigas* efflux pumps. This classification is not surprising considering that ABC transporters are well conserved across species. Most of the studies reported a strong homology between bivalve ABC pumps. For example, Huang et al. (2015) identified P-gp in the bivalve species *R. philippinarum*, *S. subcrenata* and *T. granosa* exhibiting high homology with other bivalve mollusks such as *C. ariakensis*, *C. gigas*, *M. californianus* and *M. galloprovincialis*.

Since ABCG2 transcript has also been found in hemocytes, we quantified the abundance mRNAs in both tissues. ABCG2 copy number were 2 fold higher in gills than hemocytes. This apparent disparity in gene expression over tissues has been demonstrated for other members of ABC transporters. P-gp transcripts were more abundant in gills than hemocytes in the scallop *C. farreri* (Miao et al., 2014) and the mussel *M. galloprovincialis* (Della Torre et al., 2014; Franzellitti et al., 2016). Many authors suggested that the tissue-specific expression of ABC genes is a consequence of tissue involvement in adsorption, metabolism and elimination of toxic compounds (Della Torre et al., 2014; Huang et al., 2015). The latter hypothesis may be plausible nevertheless further investigations are needed to confirm it.

4.2. ABCG2 pump efflux activity

If ABCG2 expression has been poorly described in bivalves, data on pump activity are inexistent. Herein, we explored for the first time BCRP pump activity using fluorescent probes, allocrite to human BCRP, in combination with a battery of inhibitors. In hemocytes, analysis was performed considering two major subpopulations. The first is represented by small semi granular basophils while the second includes complex granulocytes and agranular hyalinocytes (Le Foll et al., 2010). Results showed that the rate of accumulated fluorescence varied according to both cell subtypes and allocrite probes. Either in basal condition or in the presence of blockers, bodipy prazosin was more concentrated in eosinophils and inversely pheophorbide A was more stored in basophils. In appearance, these probe heterogeneous distributions may be a consequence of pronounced activity localized in particular cell subpopulation as reported by other studies. In this respect, Rioult et al. (2014) demonstrated that ABCC activity was supported by *Mytilus edulis* granulocytes. However, herein even though probes are supposed to be both allocrite to ABCG2 (Robey et al., 2004; Shi et al., 2011), their distribution profiles in hemocytes were contradictory. These discrepancies can be accounted for by to a dual effect of transporter location and differential affinity of substrates to cell compartments. According to few studies, ABC pumps can be located in mammalian lysosomal membrane in addition of plasmalemma (Rajagopal and Simon, 2003; Wioland et al., 2000). Furthermore, in mussel blood cells, it has been shown a retention of the fluorescent P-gp substrate rhodamine B in lysosomes, reversible by verapamil as blocker (Svensson et al., 2003). Another explanation to the higher accumulation of bodipy prazosin in eosinophils would be the presence of an additional pump contributing to the observed activity. Actually, if pheophorbide A has been proved to be a single substrate to mammalian ABCG2 (Robey et al., 2004), the specificity of bodipy prazosin was more discussed. Several studies reported the efflux of bodipy prazosin by

Human P-gp (Chufan et al., 2013; Kimchi-Sarfaty et al., 2002). In mussel hemocytes, the existence of an active P-gp is controversial. Classical ABCB blockers were ineffective on calcein-AM or rhodamine 123 efflux in hemocytes of *M. edulis* (Rioult et al., 2014) and *M. galloprovincialis* (Della Torre et al., 2014; Franzellitti et al., 2016). In contrast, rhodamine B efflux was inhibited by the same blockers in blood cells of the blue mussel (Svensson et al., 2003) and the freshwater painter's mussel (Zaja et al., 2006). According to these contradictory findings, the possibility of an ABCB pump interference in MXR activity cannot be excluded. It is probable that the mussel P-gp has an affinity profiles toward allocrites that differs from that of mammalian transporter and that the mussel efflux pump is capable to interact with other substrates like bodipy prazosin. Considering this latter point, a combination of allocrites and inhibitors is required to properly characterize the pump of interest.

In hemocytes, the specific blockers of mammalian BCRP, elacridar and Ko134, enhanced fluorescence level of both probes indicating an active role of ABCG2 in cell subpopulations. By contrast, sildenafil acted only on bodipy prazosin efflux and had no effect on pheophorbide A. This blocker has been described for reversing the resistance of ABCG2 and ABCB1 in Human cells (Shi et al., 2011). Surprisingly, classical inhibitors of C class transporter increased also the accumulation of fluorescent dyes. MK571 blocked the efflux of both probes while pranlukast had an effect only on pheophorbide A. Several studies used MK571 for his specific action against ABCC pump in bivalves like the blue mussel (Rioult et al., 2014), the Mediterranean mussel (Della Torre et al., 2014; Franzellitti et al., 2016), the Californian mussel (Luckenbach et al., 2008; Luckenbach and Epel, 2008) and the zebra mussel (Faria et al., 2016, 2011). However, in our study, it seems that this blocker is also able to interact with ABCG2 in mussels. Furthermore, Fischer et al. (2013) reported its action on zebrafish ABCB4. Thus, regarding this polyspecificity, results should be interpreted more carefully particularly when the tissue expresses multiple transporters.

In gills, dye accumulation was enhanced at different levels after treatment with blockers indicating a BCRP activity. Ko134 inhibited efficiently the efflux of bodipy prazosin (MAF=29±6.4) and pheophorbide A (MAF=28±7.1), whereas, MK571 blocked more bodipy prazosin (MAF=38±8.1). The difference of substrate inhibition profiles compared to hemocytes may be due to the heterogeneous distribution of the transporter in gills. Indeed, BCRP efflux activity seems to be concentrated in the anterior side of gills suggesting a localized expression of ABCG2. ABC transporter localization has been explored in few studies. P-gp was detected in apical membranes of *Mytilus galloprovincialis* gills at the tissue environment interface and

373 authors suggested his role as a barrier against entrance of xenobiotics (Luckenbach and Epel,
374 2008). Similarly, BCRP was found in apical border of mammalian tissues, (Leslie et al., 2005)
375 and *Saccostrea forskali* gills (Kingtong et al., 2007) but its exact physiological implication
376 remain unclear. Numerous studies confirmed its contribution to controlling the disposition and
377 tissue exposure of endobiotics and xenobiotics including antibiotics, sterols, immune-
378 suppressants, fluorescent dyes, photosensitizers (for review Horsey et al., 2016, Mo and Zhang
379 2012). Interestingly, ABCG2 seems also to play a role in immune modulation. Indeed, the
380 transporter participate to the differentiation of skin Langerhans cells (Van de Ven et al., 2012)
381 and myeloid dendritic cells (Jin and al., 2014). Consequently, we may think that *Mytilus edulis*
382 ABCG2 has an immune defense function in hemocytes besides the detoxification task.

383 **5. Conclusion**

384 In this study, we identified and characterized a new ABC transporter belonging to G2 subtype
385 in *Mytilus edulis*. Phylogenetic analysis revealed a sequence homology and a similar
386 organizational structure than other ABCG2 family members. Furthermore, transcripts were
387 expressed in hemocytes and with higher level in gills. Efflux activity assays show that *Mytilus*
388 *edulis* has an active BCRP protein with an heterogeneous distribution in hemocyte
389 subpopulations and gill tissues. Based on these results, it is clear that several ABC transporters
390 contribute to MXR defense system in *Mytilus edulis*. Efforts have to be made to clarify the
391 distinction between the different members and to explore their single function and specificity
392 towards allocrites and chemosensitizers.

393 **Acknowledgements**

394 This work received fundings from the State/Region Plan Contract (CPER) allocated through
395 the Research Federation FR CNRS 3730 SCALE (Sciences Appliquées à L'Environnement)
396 and from the project IPOC supported by the Agence Nationale de la Recherche “Interactions
397 between POllution and Climate changes: development of improved monitoring strategy”
398 project (ANR-12-ISV7-0004). Yosra Ben Cheikh was a recipient for a Ph.D. grant from the
399 Conseil Regional de Haute-Normandie. We thank SEBIO technical staff Aurélie Duflot for the
400 contribution.

401

402

403

404

References

Akaishi, F.M., St-Jean, S.D., Bishay, F., Clarke, J., da S Rabitto, I., de Oliveira Ribeiro, C.A., 2007. Immunological responses, histopathological finding and disease resistance of blue mussel (Mytilus edulis) exposed to treated and untreated municipal wastewater. Aquat. Toxicol. Amst. Neth. 82, 1–14. doi:10.1016/j.aquatox.2007.01.008

Anita H Poulsen, E.B.I., 2012. Chemically induced immunosuppression and disease susceptibility in marine wildlife: a literature review.

Auffret, M., Rousseau, S., Boutet, I., Tanguy, A., Baron, J., Moraga, D., Duchemin, M., 2006. A multiparametric approach for monitoring immunotoxic responses in mussels from contaminated sites in Western Mediterranea. Ecotoxicol. Environ. Saf. 63, 393–405. doi:10.1016/j.ecoenv.2005.10.016

Bard, S.M., 2000. Multixenobiotic resistance as a cellular defense mechanism in aquatic organisms. Aquat. Toxicol. 48, 357–389. doi:10.1016/S0166-445X(00)00088-6

Chen, H., Zha, J., Yuan, L., Wang, Z., 2015. Effects of fluoxetine on behavior, antioxidant enzyme systems, and multixenobiotic resistance in the Asian clam Corbicula fluminea. Chemosphere 119, 856–862. doi:10.1016/j.chemosphere.2014.08.062

Chufan, E.E., Kapoor, K., Sim, H.-M., Singh, S., Talele, T.T., Durell, S.R., Ambudkar, S.V., 2013. Multiple Transport-Active Binding Sites Are Available for a Single Substrate on Human P-Glycoprotein (ABCB1). PLOS ONE 8, e82463. doi:10.1371/journal.pone.0082463

Cooray, H.C., Janvilisri, T., van Veen, H.W., Hladky, S.B., Barrand, M.A., 2004. Interaction of the breast cancer resistance protein with plant polyphenols. Biochem. Biophys. Res. Commun. 317, 269–275. doi:10.1016/j.bbrc.2004.03.040

Dean, M., Rzhetsky, A., Allikmets, R., 2001. The human ATP-binding cassette (ABC) transporter superfamily. Genome Res. 11, 1156–1166. doi:10.1101/gr.184901

Della Torre, C., Bocci, E., Focardi, S.E., Corsi, I., 2014. Differential ABCB and ABCC gene expression and efflux activities in gills and hemocytes of Mytilus galloprovincialis and their involvement in cadmium response. Mar. Environ. Res. 93, 56–63. doi:10.1016/j.marenvres.2013.06.005

Epel, D., Luckenbach, T., Stevenson, C.N., Macmanus-Spencer, L.A., Hamdoun, A., Smital, T., 2008. EFFLUX TRANSPORTERS: Newly Appreciated Roles in Protection against Pollutants. Environ. Sci. Technol. 42, 3914–3920.

Faria, M., Navarro, A., Luckenbach, T., Piña, B., Barata, C., 2011. Characterization of the multixenobiotic resistance (MXR) mechanism in embryos and larvae of the zebra mussel (Dreissena polymorpha) and studies on its role in tolerance to single and mixture combinations of toxicants. Aquat. Toxicol. Amst. Neth. 101, 78–87. doi:10.1016/j.aquatox.2010.09.004

Faria, M., Pavlichenko, V., Burkhardt-Medicke, K., Soares, A.M.V.M., Altenburger, R., Barata, C., Luckenbach, T., 2016. Use of a combined effect model approach for discriminating between ABCB1- and ABCC1-type efflux activities in native bivalve gill tissue. Toxicol. Appl. Pharmacol. 297, 56–67. doi:10.1016/j.taap.2016.02.020

Farris, J.L., Hassel, J.H.V., 2006. Freshwater Bivalve Ecotoxicology. CRC Press.

Fischer, S., Klüver, N., Burkhardt-Medicke, K., Pietsch, M., Schmidt, A.-M., Wellner, P., Schirmer, K., Luckenbach, T., 2013. Abcb4 acts as multixenobiotic transporter and active barrier against chemical uptake in zebrafish (Danio rerio) embryos. BMC Biol. 11, 69. doi:10.1186/1741-7007-11-69

Franzellitti, S., Striano, T., Valbonesi, P., Fabbri, E., 2016. Insights into the regulation of the MXR response in haemocytes of the Mediterranean mussel (Mytilus galloprovincialis). Fish Shellfish Immunol. 58, 349–358. doi:10.1016/j.fsi.2016.09.048

Giarratano, E., Duarte, C.A., Amin, O.A., 2010. Biomarkers and heavy metal bioaccumulation in mussels transplanted to coastal waters of the Beagle Channel. Ecotoxicol. Environ. Saf. 73, 270–279. doi:10.1016/j.ecoenv.2009.10.009

Gottesman, M.M., Ling, V., 2006. The molecular basis of multidrug resistance in cancer: the early years of P-glycoprotein research. FEBS Lett. 580, 998–1009. doi:10.1016/j.febslet.2005.12.060

Gupta, S.K., Singh, J., 2011. Evaluation of mollusc as sensitive indicatior of heavy metal pollution in aquatic system: A review. IIOAB J. 2, 49–57.

Haberkorn, H., Tran, D., Massabuau, J.-C., Ciret, P., Savar, V., Soudant, P., 2011. Relationship between valve activity, microalgae concentration in the water and toxin accumulation in the digestive gland of the Pacific oyster Crassostrea gigas exposed to Alexandrium minutum. Mar. Pollut. Bull. 62, 1191–1197. doi:10.1016/j.marpolbul.2011.03.034

Hégaret, H., Wikfors, G.H., Shumway, S.E., 2007. Diverse feeding responses of five species of bivalve mollusc when exposed to three species of harmful algae. J. Shellfish Res. 26, 549–559. doi:10.2983/0730-8000(2007)26[549:DFROFS]2.0.CO;2

Horsey, A.J., Cox, M.H., Sarwat, S., Kerr, I.D., 2016. The multidrug transporter ABCG2: still more questions than answers. Biochem. Soc. Trans. 44, 824–830. doi:10.1042/BST20160014

Huang, L., Liu, S.-L., Zheng, J.-W., Li, H.-Y., Liu, J.-S., Yang, W.-D., 2015. P-glycoprotein and its inducible expression in three bivalve species after exposure to Prorocentrum lima. Aquat. Toxicol. Amst. Neth. 169, 123–132. doi:10.1016/j.aquatox.2015.10.012

Huang, L., Wang, J., Chen, W.-C., Li, H.-Y., Liu, J.-S., Jiang, T., Yang, W.-D., 2014. P-glycoprotein expression in Perna viridis after exposure to Prorocentrum lima, a dinoflagellate producing DSP toxins. Fish Shellfish Immunol. 39, 254–262. doi:10.1016/j.fsi.2014.04.020

Jin, J.-O., Zhang, W., Wong, K.-W., Kwak, M., van Driel, I.R., Yu, Q., 2014. Inhibition of Breast Cancer Resistance Protein (ABCG2) in Human Myeloid Dendritic Cells Induces Potent Tolerogenic Functions during LPS Stimulation. PLoS ONE 9. doi:10.1371/journal.pone.0104753

Kathawala, R.J., Gupta, P., Ashby, C.R., Chen, Z.-S., 2015. The modulation of ABC transporter-mediated multidrug resistance in cancer: a review of the past decade. Drug Resist. Updat. Rev. Comment. Antimicrob. Anticancer Chemother. 18, 1–17. doi:10.1016/j.drup.2014.11.002

Kimchi-Sarfaty, C., Gribar, J.J., Gottesman, M.M., 2002. Functional Characterization of Coding Polymorphisms in the HumanMDR1 Gene Using a Vaccinia Virus Expression System. Mol. Pharmacol. 62, 1–6. doi:10.1124/mol.62.1.1

Kingtong, S., Chitramvong, Y., Janvilisri, T., 2007. ATP-binding cassette multidrug transporters in Indian-rock oyster Saccostrea forskali and their role in the export of an environmental organic pollutant tributyltin. Aquat. Toxicol. 85, 124–132. doi:10.1016/j.aquatox.2007.08.006

Köhler, A., Lauritzen, B., Jansen, D., Böttcher, P., Teguliwa, L., Krüner, G., Broeg, K., 1998. Detection of P-glycoprotein mediated MDR/MXR in Caranus maenas hepatopancreas by immuno-gold-silver labeling. Mar. Environ. Res., Pollutant Responses in Marine Organisms 46, 411–414. doi:10.1016/S0141-1136(97)00069-X

Kurelec, B., 1992. The multixenobiotic resistance mechanism in aquatic organisms. Crit. Rev. Toxicol. 22, 23–43. doi:10.3109/10408449209145320

Kurelec, B., Krca, S., Pivcevic, B., Ugarković, D., Bachmann, M., Imsiecke, G., Müller, W.E., 1992. Expression of P-glycoprotein gene in marine sponges. Identification and characterization of the 125 kDa drug-binding glycoprotein. Carcinogenesis 13, 69–76.

505 Kurelec, B., Pivcević, B., 1989. Distinct glutathione-dependent enzyme activities and a
506 verapamil-sensitive binding of xenobiotics in a fresh-water mussel Anodonta cygnea.
507 Biochem. Biophys. Res. Commun. 164, 934–940.
508 Lacroix, C., Coquillé, V., Guyomarch, J., Auffret, M., Moraga, D., 2014. A selection of
509 reference genes and early-warning mRNA biomarkers for environmental monitoring
510 using *Mytilus* spp. as sentinel species. Mar. Pollut. Bull. 86, 304–313.
511 Le Foll, F., Rioult, D., Boussa, S., Pasquier, J., Dagher, Z., Leboulenger, F., 2010.
512 Characterisation of Mytilus edulis hemocyte subpopulations by single cell time-lapse
513 motility imaging. Fish Shellfish Immunol. 28, 372–386. doi:10.1016/j.fsi.2009.11.011
514 Lebedeva, I.V., Pande, P., Patton, W.F., 2011. Sensitive and Specific Fluorescent Probes for
515 Functional Analysis of the Three Major Types of Mammalian ABC Transporters.
516 PLoS ONE 6, e22429. doi:10.1371/journal.pone.0022429
517 Lepist, E.-I., Phan, T.K., Roy, A., Tong, L., Maclennan, K., Murray, B., Ray, A.S., 2012.
518 Cobicistat boosts the intestinal absorption of transport substrates, including HIV
519 protease inhibitors and GS-7340, in vitro. Antimicrob. Agents Chemother. 56, 5409–
520 5413. doi:10.1128/AAC.01089-12
521 Leslie, E.M., Deeley, R.G., Cole, S.P.C., 2005. Multidrug resistance proteins: role of P-
522 glycoprotein, MRP1, MRP2, and BCRP (ABCG2) in tissue defense. Toxicol. Appl.
523 Pharmacol. 204, 216–237. doi:10.1016/j.taap.2004.10.012
524 Linton, K.J., 2007. Structure and Function of ABC Transporters. Physiology 22, 122–130.
525 doi:10.1152/physiol.00046.2006
526 Luckenbach, T., Altenburger, R., Epel, D., 2008. Teasing apart activities of different types of
527 ABC efflux pumps in bivalve gills using the concepts of independent action and
528 concentration addition. Mar. Environ. Res. 66, 75–76.
529 doi:10.1016/j.marenvres.2008.02.027
530 Luckenbach, T., Epel, D., 2008. ABCB- and ABCC-type transporters confer multixenobiotic
531 resistance and form an environment-tissue barrier in bivalve gills. Am. J. Physiol.
532 Regul. Integr. Comp. Physiol. 294, R1919-1929. doi:10.1152/ajpregu.00563.2007
533 Luedeking, A., Koehler, A., 2002. Identification of six mRNA sequences of genes to
534 multixenobiotic resistance (MXR) and biotransformation in Mytilus edulis. Mar.
535 Ecol.-Prog. Ser. - MAR ECOL-PROGR SER 238, 115–124. doi:10.3354/meps238115
536 Luedeking, A., Van Noorden Cornelis J. F., Koehler A., 2005. Identification and
537 characterisation of a multidrug resistance-related protein mRNA in the blue mussel
538 Mytilus edulis. MEPS 286,167-175. doi:10.3354/meps286167.
539 McFadzen, I., Eufemia, N., Heath, C., Epel, D., Moore, M., Lowe, D., 2000. Multidrug
540 resistance in the embryos and larvae of the mussel Mytilus edulis. Mar. Environ. Res.
541 50, 319–323.
542 Miao, J., Cai, Y., Pan, L., Li, Z., 2014. Molecular cloning and characterization of a MXR-
543 related P-glycoprotein cDNA in scallop Chlamys farreri: transcriptional response to
544 benzo(a)pyrene, tetrabromobisphenol A and endosulfan. Ecotoxicol. Environ. Saf.
545 110, 136–142. doi:10.1016/j.ecoenv.2014.08.029
546 Minier, C., Forget-Leray, J., Bjørnstad, A., Camus, L., 2008. Multixenobiotic resistance,
547 acetyl-choline esterase activity and total oxyradical scavenging capacity of the Arctic
548 spider crab, Hyasaraneus, following exposure to bisphenol A, tetra bromo diphenyl
549 ether and diallyl phthalate. Mar. Pollut. Bull. 56, 1410–1415.
550 doi:10.1016/j.marpolbul.2008.05.005
551 Mo, W., Zhang, J.-T., 2011. Human ABCG2: structure, function, and its role in multidrug
552 resistance. Int. J. Biochem. Mol. Biol. 3, 1–27.

553 Murgarella, M., Puiu, D., Novoa, B., Figueras, A., Posada, D., Canchaya, C., 2016. A First
554 Insight into the Genome of the Filter-Feeder Mussel Mytilus galloprovincialis. PLOS
555 ONE 11, e0151561. doi:10.1371/journal.pone.0151561
556 Nagayama, S., Chen, Z.S., Kitazono, M., Takebayashi, Y., Niwa, K., Yamada, K., Tani, A.,
557 Haraguchi, M., Sumizawa, T., Furukawa, T., Aikou, T., Akiyama, S., 1998. Increased
558 sensitivity to vincristine of MDR cells by the leukotriene D4 receptor antagonist,
559 ONO-1078. Cancer Lett. 130, 175–182.
560 Navarro, A., Weißbach, S., Faria, M., Barata, C., Piña, B., Luckenbach, T., 2012. Abcb and
561 Abcc transporter homologs are expressed and active in larvae and adults of zebra
562 mussel and induced by chemical stress. Aquat. Toxicol. Amst. Neth. 122–123, 144–
563 152. doi:10.1016/j.aquatox.2012.06.008
564 Nielsen, D., Skovsgaard, T., 1992. P-glycoprotein as multidrug transporter: a critical review
565 of current multidrug resistant cell lines. Biochim. Biophys. Acta 1139, 169–183.
566 Olson, D.P., Taylor, B.J., Ivy, S.P., 2001. Detection of MRP functional activity: calcein AM
567 but not BCECF AM as a Multidrug Resistance-related Protein (MRP1) substrate.
568 Cytometry 46, 105–113.
569 Rajagopal, A., Simon, S.M., 2003. Subcellular Localization and Activity of Multidrug
570 Resistance Proteins. Mol. Biol. Cell 14, 3389–3399. doi:10.1091/mbc.E02-11-0704
571 Rioult, D., Pasquier, J., Boulangé-Lecomte, C., Poret, A., Abbas, I., Marin, M., Minier, C., Le
572 Foll, F., 2014. The multi-xenobiotic resistance (MXR) efflux activity in hemocytes of
573 Mytilus edulis is mediated by an ATP binding cassette transporter of class C (ABCC)
574 principally inducible in eosinophilic granulocytes. Aquat. Toxicol. Amst. Neth. 153,
575 98–109. doi:10.1016/j.aquatox.2013.11.012
576 Robey, R.W., Steadman, K., Polgar, O., Morisaki, K., Blayney, M., Mistry, P., Bates, S.E.,
577 2004. Pheophorbide a is a specific probe for ABCG2 function and inhibition. Cancer
578 Res. 64, 1242–1246.
579 Sarkadi, B., Homolya, L., Szakács, G., Váradi, A., 2006. Human multidrug resistance ABCB
580 and ABCG transporters: participation in a chemoimmunity defense system. Physiol.
581 Rev. 86, 1179–1236. doi:10.1152/physrev.00037.2005
582 Sato, H., Siddig, S., Uzu, M., Suzuki, S., Nomura, Y., Kashiba, T., Gushimiyagi, K., Sekine,
583 Y., Uehara, T., Arano, Y., Yamaura, K., Ueno, K., 2015. Elacridar enhances the
584 cytotoxic effects of sunitinib and prevents multidrug resistance in renal carcinoma
585 cells. Eur. J. Pharmacol. 746, 258–266. doi:10.1016/j.ejphar.2014.11.021
586 Sharom, F.J., 2008. ABC multidrug transporters: structure, function and role in
587 chemoresistance. Pharmacogenomics 9, 105–127. doi:10.2217/14622416.9.1.105
588 Shi, Z., Tiwari, A.K., Shukla, S., Robey, R.W., Singh, S., Kim, I.-W., Bates, S.E., Peng, X.,
589 Abraham, I., Ambudkar, S.V., Talele, T.T., Fu, L.-W., Chen, Z.-S., 2011. Sildenafil
590 reverses ABCB1- and ABCG2-mediated chemotherapeutic drug resistance. Cancer
591 Res. 71, 3029–3041. doi:10.1158/0008-5472.CAN-10-3820
592 Svensson, S., Särngren, A., Förlin, L., 2003. Mussel blood cells, resistant to the cytotoxic
593 effects of okadaic acid, do not express cell membrane p-glycoprotein activity
594 (multixenobiotic resistance). Aquat. Toxicol. Amst. Neth. 65, 27–37.
595 Toomey, B.H., Epel, D., 1993. Multixenobiotic Resistance in Urechis caupo Embryos:
596 Protection From Environmental Toxins. Biol. Bull. 185, 355–364.
597 Van de Ven, R., Lindenberg, J.J., Reurs, A.W., Scheper, R.J., Scheffer, G.L., de Gruijl, T.D.,
598 2012. Preferential Langerhans cell differentiation from CD34(+) precursors upon
599 introduction of ABCG2 (BCRP). Immunol. Cell Biol. 90, 206–215.
600 doi:10.1038/icb.2011.25
601 Wioland, M.A., Fleury-Feith, J., Corlieu, P., Commo, F., Monceaux, G., Lacau-St-Guily, J.,
602 Bernaudin, J.F., 2000. CFTR, MDR1, and MRP1 immunolocalization in normal

human nasal respiratory mucosa. J. Histochem. Cytochem. Off. J. Histochem. Soc. 48, 1215–1222.

Xuereb, B., Forget-Leray, J., Souissi, S., Glippa, O., Devreker, D., Lesueur, T., Marie, S., Danger, J.-M., Boulangé-Lecomte, C., 2012. Molecular characterization and mRNA expression of grp78 and hsp90A in the estuarine copepod Eurytemora affinis. Cell Stress Chaperones. doi:10.1007/s12192-012-0323-9

Zaja, R., Klobucar, G.I.V., Sauerborn Klobucar, R., Hackenberger, B.K., Smital, T., 2006. Haemolymph as compartment for efficient and non-destructive determination of P-glycoprotein (Pgp) mediated MXR activity in bivalves. Comp. Biochem. Physiol. Toxicol. Pharmacol. CBP 143, 103–112. doi:10.1016/j.cbpc.2005.12.009

627 **Figure legend**

628 **Figure 1.** Topology of the *Mytilus edulis* ABCG2 protein with membrane spanning domains
629 (MSD) as predicted by TMHMM v2.0 and nucleotide binding domain (NBD) indicated by the
630 Walkers A and B, the C motif, the Q-, D- and H-loops. GS marks the N-glycosylation sites.

631 **Figure 2.** ClustalW alignments of *Mytilus edulis* ABCG2 with human ABCG2 transporter
632 (GenBank accession no. Q9UNQ0). Conserved Walker A and B motifs, the ABC signature C
633 motif, Q-, D- and H-loops are indicated with coloured boxes. Underlined sections represent
634 transmembrane helices according to the TMHMM program. GS marks the N-glycosylation
635 sites. * indicate similar amino acid

636 **Figure 3**. Phylogenetic tree based on multiple alignment (ClustalX) of various ABCG2
637 transporter subtype sequences from diverse vertebrates and invertebrates. Tree was generated
638 using the neighbour-joining method, distances are shown at the nodes.

639 **Figure 4**. Relative expression of *abcg2*-like in *Mytilus edulis* hemocytes and gills.
640 Transcript levels are normalized to *ef1α* (hk gene). Letters indicate significant differences
641 (mean ± SEM, n=5, $p<0.01$, Student's t-test).

642 **Figure 5**. Flow cytometry analysis of BCRP efflux activity in hemocyte subpopulations.
643 Cells were preincubated for 30 min with various blockers at 30 µM and then a fluorescent dye,
644 bodipy prazosin (0.5 µM) or pheophorbide A (5µM), was loaded for 15 min. ***a***, dot plot of cell
645 Coulter-type electronic volume (EV), graphed versus cell complexity side-scatter (SS). Two
646 subpopulations of interest have been delimited by off-line analysis and considered to
647 correspond to basophils and eosinophils. ***b***, normalized fluorescence (FL1-FC, for FL1-
648 fluorescence concentration) distributions of the sample presented in *a*, expressed as the ratio of
649 FL1 to cell size. ***c***, mean fluorescence of hemocytes in absence or presence of blockers, for
650 respective fluorescent dyes (bars are SEM, n=3-5). * indicates significant differences from the
651 control (Student's t-test, *$p<0.05$) and § marks differences between hemocyte subpopulations
652 (Student's t-test, §$p<0.05$)

653 **Figure 6.** BCRP efflux activity in gills measured by dye accumulation in presence of ABC
654 transporter inhibitors. Cells were preincubated for 30 min with various blockers at 30 µM and
655 then a fluorescent dye, bodipy prazosin (0.5 µM) or pheophorbide A (5µM), was loaded for 15
656 min. ***a***, mean of fluorescence of gills in absence or presence of blockers and, for respective
657 fluorescent dyes (bars are SEM, n=4, *$p<0.05$ Student's t-test). *b*, colour-coded cartography of

probes accumulation in gills in control and blocked samples (P: posterior, A:anterior, DS: Dorsal side, VS: Ventral side)

Tables:

Table 1. Specificity of ABC blockers used in this study

Chemicals	Blocker specificity	Reference
Sildenafil	ABCB/ABCG2	Shi et al., 2011
MK571	ABCC	Olson et al., 2001
Pranlukast (ONO-1078)	ABCC	Nagayama et al., 1998
Ko134	ABCG2	Lepist et al., 2012
Elacridar	ABCG2	Sato et al., 2015

Table 2. Primers used in this study

Gene	Accession number	Fw 5'-3'	Rev 5'-3'	Tm (°C)	Amplicon size (pb)	Reaction
abcg2	gi|406717747	CCCTGCTGGTTTAAGTGGAC	ATCAACACCAACCACTGCAT	59	879	PCR
	KX551963	GCGAGATGGACAAACGAACC	ATGGATTTGGTCCTTGCACT	60	2248	PCR
	KX551963	TGGTGGGCTATGTTGTTCAGGATGA	CTTTCTCCACCAGATACACCACGGA	64	214	RACE PCR
	KX551963	TGTGCTATTTTTAGATGAACCAACA	TCCTTCCTTTTAATGCTAATCTTCTC	59	95	qPCR
ef1α	AF063420.1	TGTGCTATTTTTAGATGAACCAACA	TCCTTCCTTTTAATGCTAATCTTCTC	59	61	qPCR

Table 3.Comparison of BCRP activity detection in hemocyte subpopulations using BCRP probes and inhibitors of different specificity

BCRP Probe	Hemocyte subpopulation	Sildenafil	MK571	Ko134	Elacridar	Pranlukast
Bodipy prazosin	Basophils	55 ± 6.9	38 ± 11.7	25 ± 9.9	44 ± 5.3	0
	Eosinophils	53 ± 2.5	39 ± 5.6	32 ± 1.3	46 ± 2.5	0
Pheophorbide A	Basophils	9 ± 8.6	35 ± 11.9	35 ± 15.8	21 ± 13.6	36 ± 12.1
	Eosinophils	18 ± 12.3	50 ± 8.3	41 ± 14.7	25 ± 12.5	41 ± 12.6

Average MAF values ± SEM for three (for pheophorbide A) and five (for bodipy prazosin) representative experiments are provided. Negative MAF values have been replaced with 0.

Table 4. Comparison of BCRP activity detection gills using BCRP probes and inhibitors of different specificity

BCRP Probe	Sildenafil	MK571	Ko134	Elacridar	Pranlukast
Bodipy prazosin	12 ± 8.3	38 ± 8.1	29 ± 6.4	18 ± 7.2	17 ± 10.5
Pheophorbide A	22 ± 4.2	13 ± 8	28 ± 7.1	17 ± 4.9	6 ± 15.2

Average MAF values ± SEM for four representative experiments are provided. Negative MAF values have been replaced with 0.

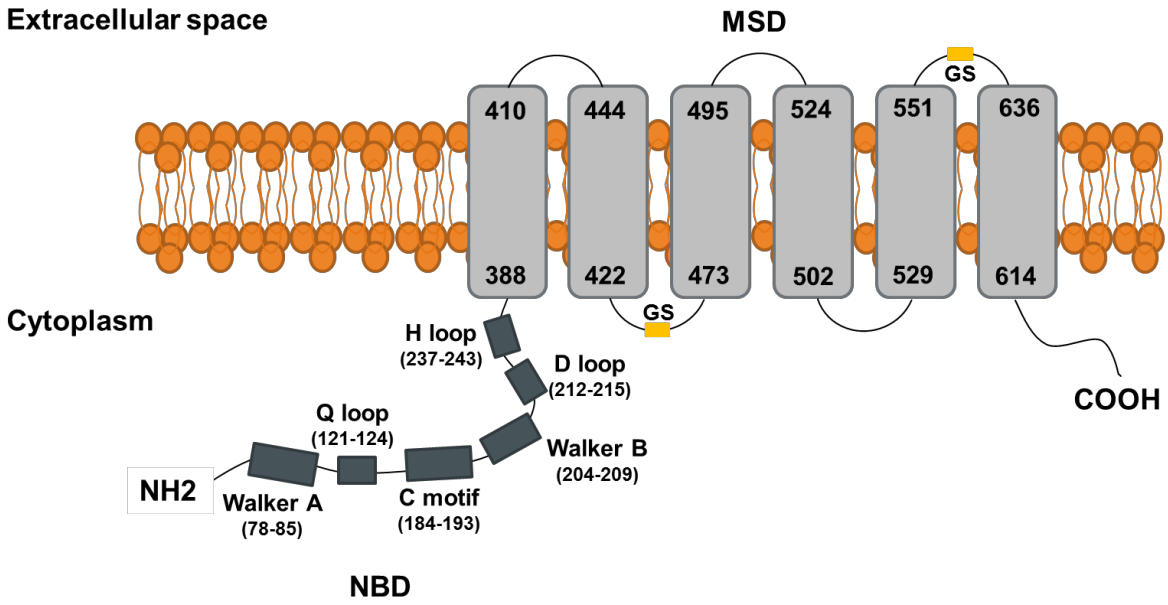
Extracellular space
MSD
GS
410
444
495
524
551
636
388
422
473
502
529
614
Cytoplasm
GS
H loop
(237-243)
D loop
(212-215)
COOH
Q loop
(121-124)
Walker B
(204-209)
NH2
Walker A
(78-85)
C motif
(184-193)
NBD

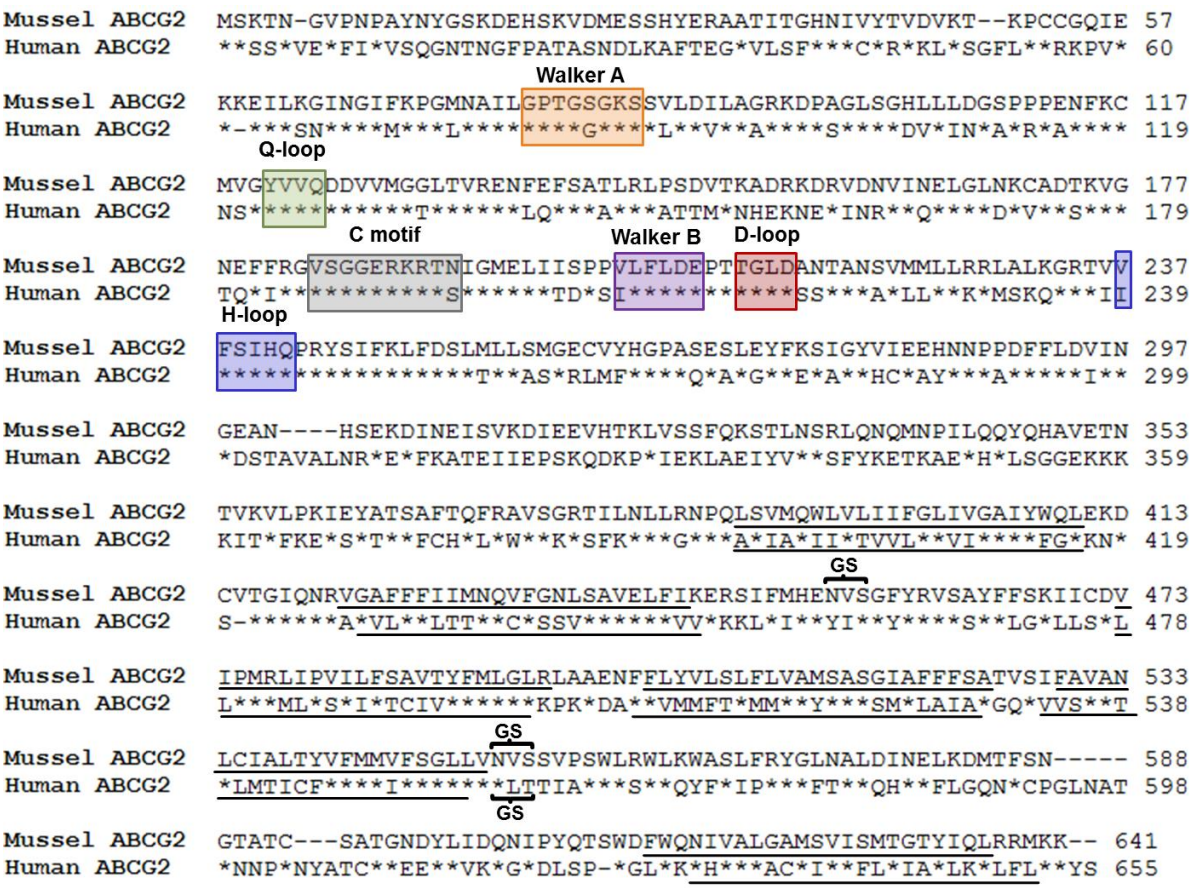
Mussel ABCG2 MSKTN-GVPNPAYNYGSKDEHSKVDMESSHYERAATITGHNIVYTVDVKT--KPCCGQIE 57
Human ABCG2 **SS*VE*FI*VSQGNTNGFPATASNDLKAFTEG*VLSF***C*R*KL*SGFL**RKPV* 60
Walker A
Mussel ABCG2 KKEILKGINGIFKPGMNAILGPTGSGKSSVLDILAGRKDPAGLSGHLLLDGSPPPENFKC 117
Human ABCG2 *-***SN****M***L*********G***L**V**A****S****DV*IN*A*R*A**** 119
Q-loop
Mussel ABCG2 MVGYVVQDDVVMGGLTVRENFEFSATLRLPSDVTKADRKDRVDNVINELGLNKCADTKVG 177
Human ABCG2 NS*****************T******LQ***A***ATTM*NHEKNE*INR**Q****D*V**S*** 179
C motif
Walker B
D-loop
Mussel ABCG2 NEFFRGVSGGERKRTNIGMELIISPPVLFLDEPTTGLDANTANSVMMLLRRLALKGRTVV 237
Human ABCG2 TQ*I**********S******TD*SI*********SS***A*LL**K*MSKQ***II 239
H-loop
Mussel ABCG2 FSIHQPRYSIFKLFDSLMLLSMGECVYHGPASESLEYFKSIGYVIEEHNNPPDFFLDVIN 297
Human ABCG2 ******************T**AS*RLMF****Q*A*G**E*A**HC*AY***A*****I** 299
Mussel ABCG2 GEAN----HSEKDINEISVKDIEEVHTKLVSSFQKSTLNSRLQNQMNPILQQYQHAVETN 353
Human ABCG2 *DSTAVALNR*E*FKATEIIEPSKQDKP*IEKLAEIYV**SFYKETKAE*H*LSGGEKKK 359
Mussel ABCG2 TVKVLPKIEYATSAFTQFRAVSGRTILNLLRNPQLSVMQWLVLIIFGLIVGAIYWQLEKD 413
Human ABCG2 KIT*FKE*S*T**FCH*L*W**K*SFK***G***A*IA*II*TVVL**VI****FG*KN* 419
GS
Mussel ABCG2 CVTGIQNRVGAFFFIIMNQVFGNLSAVELFIKERSIFMHENVSGFYRVSAYFFSKIICDV 473
Human ABCG2 S-******A*VL**LTT**C*SSV******VV*KKL*I**YI**Y****S**LG*LLS*L 478
Mussel ABCG2 IPMRLIPVILFSAVTYFMLGLRLAAENFFLYVLSLFLVAMSASGIAFFFSATVSIFAVAN 533
Human ABCG2 L***ML*S*I*TCIV******KPK*DA**VMMFT*MM**Y***SM*LAIA*GQ*VVS**T 538
GS
Mussel ABCG2 LCIALTYVFMMVFSGLLVNVSSVPSWLRWLKWASLFRYGLNALDINELKDMTFSN----- 588
Human ABCG2 *LMTICF****I*******LTTIA***S**QYF*IP***FT**QH**FLGQN*CPGLNAT 598
GS
Mussel ABCG2 GTATC---SATGNDYLIDQNIPYQTSWDFWQNIVALGAMSVISMTGTYIQLRRMKK-- 641
Human ABCG2 *NNP*NYATC**EE**VK*G*DLSP-*GL*K*H***AC*I**FL*IA*LK*LFL**YS 655

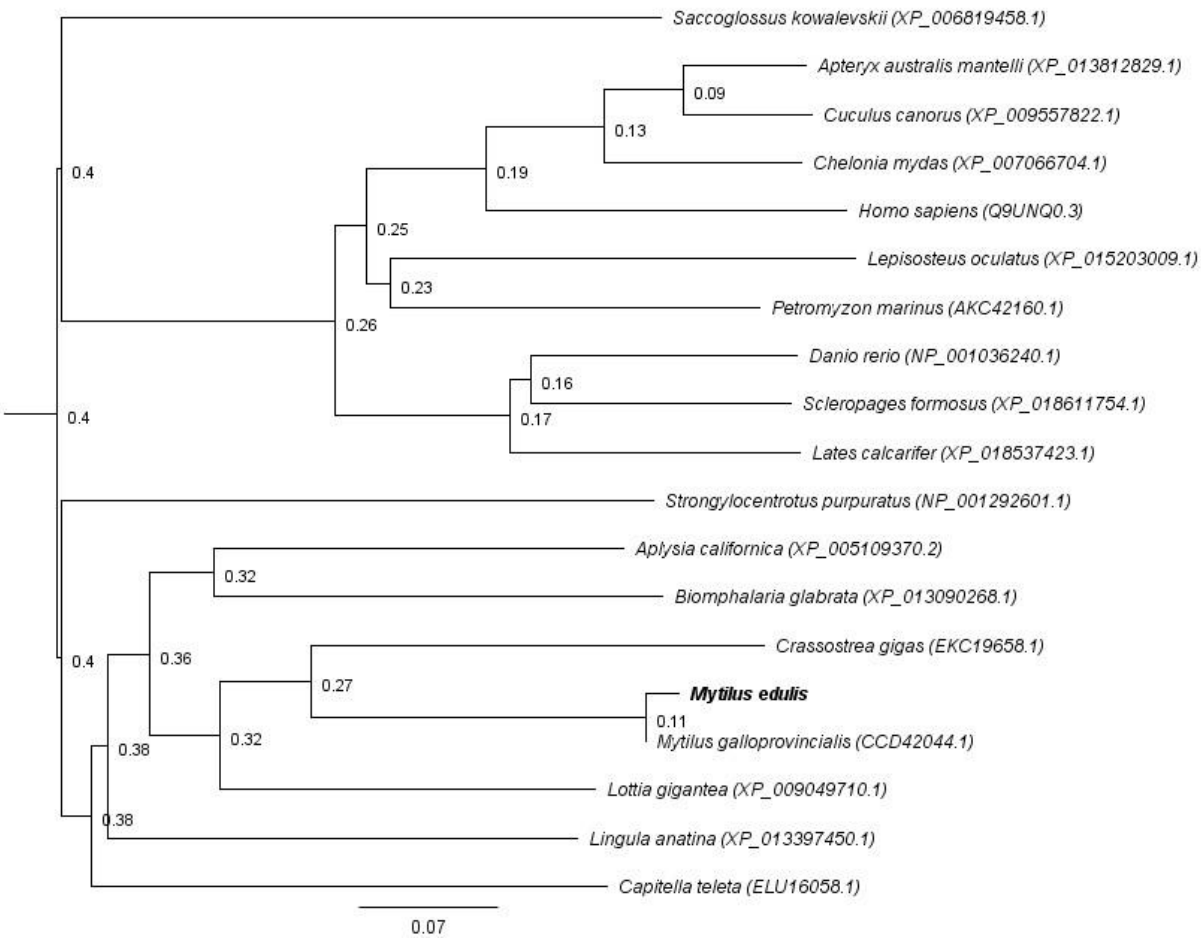
Saccoglossus kowalevskii (XP_006819458.1)
Apteryx australis mantelli (XP_013812829.1)
0.09
Cuculus canorus (XP_009557822.1)
0.13
Chelonia mydas (XP_007066704.1)
0.19
Homo sapiens (Q9UNQ0.3)
0.4
0.25
Lepisosteus oculatus (XP_015203009.1)
0.23
Petromyzon marinus (AKC42160.1)
0.26
Danio rerio (NP_001036240.1)
0.16
Scleropages formosus (XP_018611754.1)
0.4
0.17
Lates calcarifer (XP_018537423.1)
Strongylocentrotus purpuratus (NP_001292601.1)
Aplysia californica (XP_005109370.2)
0.32
Biomphalaria glabrata (XP_013090268.1)
Crassostrea gigas (EKC19658.1)
0.4
0.36
0.27
Mytilus edulis
0.11
Mytilus galloprovincialis (CCD42044.1)
0.38
0.32
Lottia gigantea (XP_009049710.1)
0.38
Lingula anatina (XP_013397450.1)
Capitella teleta (ELU16058.1)
0.07

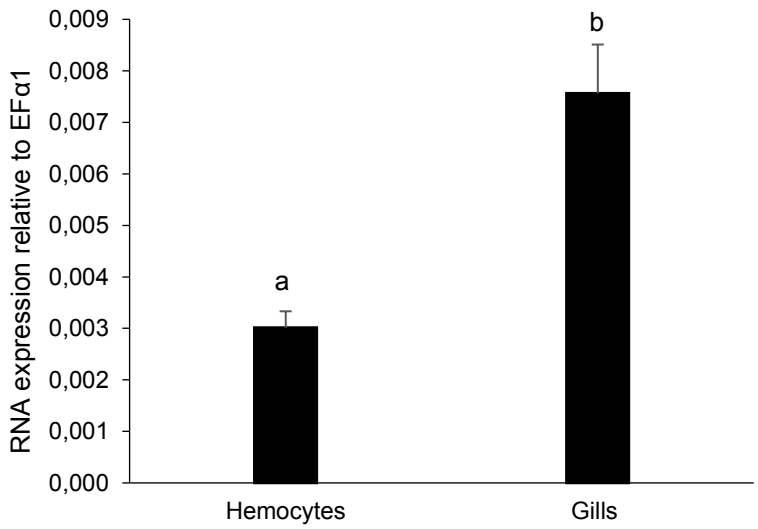
RNA expression relative to EFα1
0,009
0,008
0,007
0,006
0,005
0,004
0,003
0,002
0,001
0,000
a
b
Hemocytes
Gills

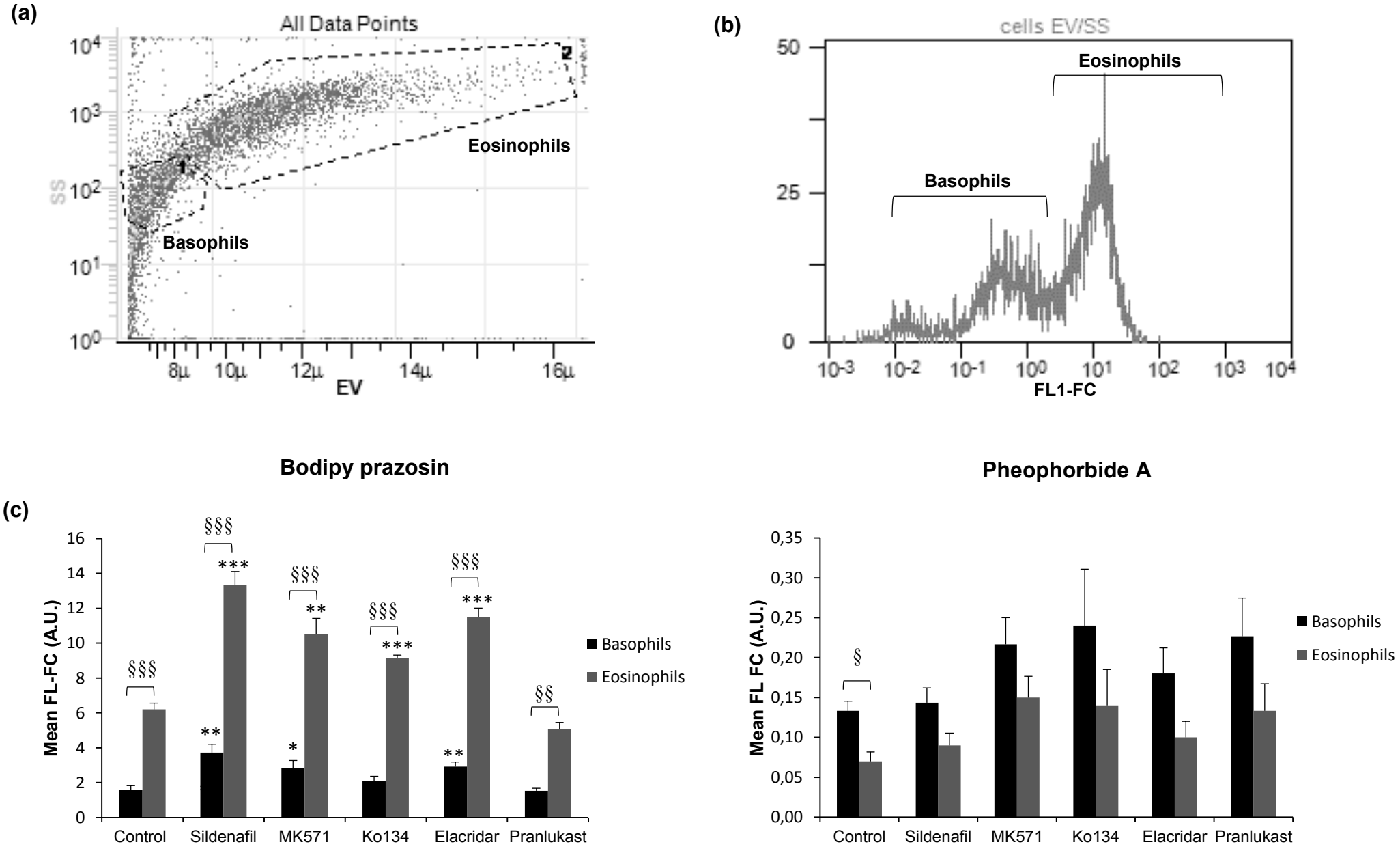
(a)
All Data Points
SS
EV
Basophils
Eosinophils
(b)
cells EV/SS
Basophils
Eosinophils
FL1-FC
Bodipy prazosin
(c)
Mean FL-FC (A.U.)
Control
Sildenafil
MK571
Ko134
Elacridar
Pranlukast
Basophils
Eosinophils
Pheophorbide A
Mean FL FC (A.U.)

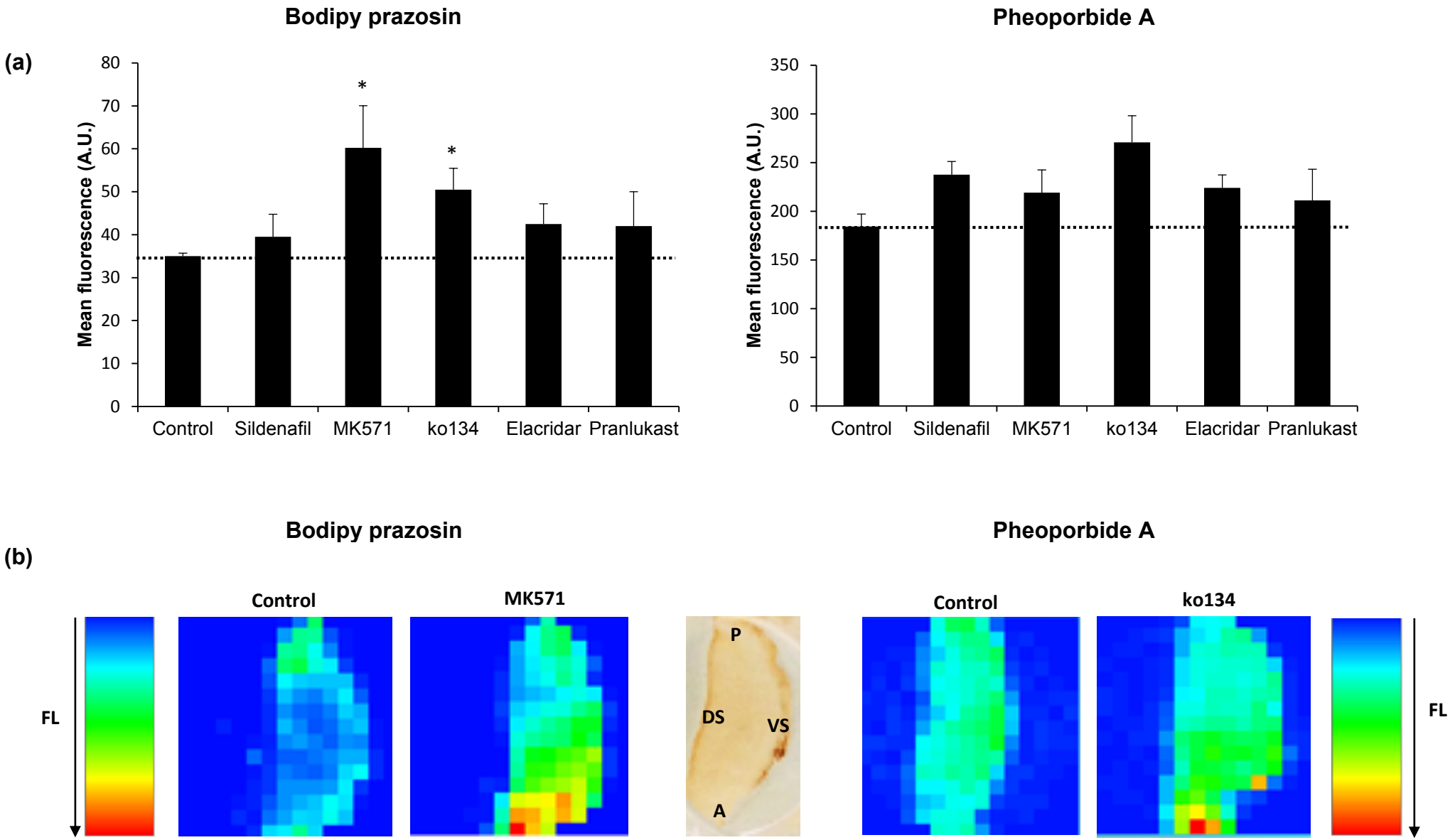
(a)
Bodipy prazosin
Mean fluorescence (A.U.)
80
70
60
50
40
30
20
10
0
*
*
Control
Sildenafil
MK571
ko134
Elacridar
Pranlukast
Pheoporbide A
Mean fluorescence (A.U.)
350
300
250
200
150
100
50
0
Control
Sildenafil
MK571
ko134
Elacridar
Pranlukast
(b)
Bodipy prazosin
Control
MK571
FL
P
DS
VS
A
Pheoporbide A
Control
ko134
FL